Journal of Physics B: Atomic, Molecular and Optical Physics

Phase transition of the ground state for two-component Bose–Einstein condensates in a triple-well trap

IOP PUBLISHING JOURNAL OF PHYSICS B: ATOMIC, MOLECULAR AND OPTICAL PHYSICS

J. Phys. B: At. Mol. Opt. Phys. **44** (2011) 115301 (6pp) doi:10.1088/0953-4075/44/11/115301

Phase transition of the ground state for two-component Bose–Einstein condensates in a triple-well trap

Xin Jiang[1,2], **Li-Bin Fu**[2,3], **Wen-shan Duan**[1] **and Jie Liu**[2,3]

[1] Physics and Electronic Engineering College, Northwest Normal University, 730070 Lanzhou, People's Republic of China
[2] Science and Technology Computation Physics Laboratory, Institute of Applied Physics and Computational Mathematics, 100088 Beijing, People's Republic of China
[3] Center for Applied Physics and Technology, Peking University, 100084 Beijing, People's Republic of China

E-mail: liu_jie@iapcm.ac.cn

Received 17 November 2010, in final form 3 April 2011
Published 17 May 2011
Online at stacks.iop.org/JPhysB/44/115301

Abstract
We consider the ground-state structure of two-component Bose–Einstein condensates trapped in a triple-well potential. We observe three structural phases of self-trapping, phase separation and symmetry state phase, which reflect the interplay of the intraspecies and interspecies interactions. We also show that the transitions from the self-trapping phase to the symmetry phase and from the phase separation to the symmetry phase are first-order phase transitions, while the transition from the self-trapping phase to the phase separation phase is a continuous one.

1. Introduction

Phase transition and coexistence of different phases in a multi-component system are of great importance to many areas of physics, chemistry and biology. An ideal system to study these phenomena is a multi-component dilute atomic gas mixture of Bose–Einstein condensates (BECs) at zero temperature, due to the simplicity of its theoretical description. Multi-component BECs have been extensively studied over the last few years [1–19]. Many interesting effects have been experimentally determined and theoretically predicted, including phase transitions and symmetry breaking [2], effects produced by a phase difference between components [3], stability properties [4], Josephson oscillations [5], four-wave mixing [6], and trapping of boson–fermion and fermion–fermion systems [7].

A large variety of different species can be used to produce mixtures of condensed bosons. Mixtures of two different elements [8], or of different isotopes of the same element [9], or simply different hyperfine states of the same atom [10, 11], can be considered. The tunability of inter-species and intra-species interactions [12] via magnetic and optical Feshbach resonances makes the mixture of BECs a very attractive candidate for exploring a new phenomenon involving quantum coherence and nonlinearity in a multi-component system. Lots of studies consider multi-component BECs in a two-well system (dimer) and reveal many interesting phenomena, e.g., quantum-correlated tunnelling between the two species [13], the renewed macroscopic Josephson oscillations and self-trapping effects [14, 15], the spin tunnelling [16, 17], stability [18], measure synchronization [19], etc. The richness of the results provides motivation to go beyond the two-well system and consider new scenarios where even a richer phenomenon should be observed. The three-well (trimer) opens new exciting opportunities; many studies have been carried out with the single-component BECs in a three-well trap [20–22].

In this paper, we consider the two-component BECs in a trimer system and study the structural changes of the ground state with the experimentally controlled parameters U_a (U_b) (intraspecies interaction strength) and U_{ab} (the interspecies interaction strength). It is noted that there are three regions in the phase space for this system corresponding to the symmetry state (SS) phase, self-trapping (ST) phase and phase separation (PS) phase, respectively, which depend on the parameters of interaction strength. The self-trapped phase is referred to as the stable state, in which the atoms occupy different wells with unequal probabilities. These kinds of self-trapped states were widely used to describe the unequal occupation of atoms in each well due to nonlinearity [23–28].

Two kinds of phase transitions are found. From ST and PS to SS, the transitions are the first-order phase transitions, while from ST to PS, the transition is a continuous phase transition.

The paper is organized as follows. In section 2, a model is proposed. In section 3, the numerical results are given. Two kinds of phase transitions are found. In section 4, conclusions are given.

2. Model

We consider two-component BECs trapped in a symmetrical triple well. The Hamiltonian of such a system is given by

$$H = -\sum_{\langle i,j\rangle}\left[T_a\left(\hat{a}_i^\dagger\hat{a}_j + \hat{a}_j^\dagger\hat{a}_i\right) + T_b\left(\hat{b}_i^\dagger\hat{b}_j + \hat{b}_j^\dagger\hat{b}_i\right)\right] + \frac{1}{2}U_a\sum_i\hat{n}_{ai}^2 + \frac{1}{2}U_b\sum_i\hat{n}_{bi}^2 + U_{ab}\sum_i\hat{n}_{ai}\hat{n}_{bi} \tag{1}$$

where the subscripts i ($i = 1, 2, 3$) specify the three wells, a and b refer to two different components, the operators $\hat{a}_i^\dagger(\hat{a}_i)$ and $\hat{b}_i^\dagger(\hat{b}_i)$, which obey the canonical commutation relations $\left[\hat{a}_i(\hat{b}_i), \hat{a}_j^\dagger(\hat{b}_j)\right] = \delta_{ij}$, generate (annihilate) a boson of components a and b in the ith well, respectively, $\hat{n}_{ai} = \hat{a}_i^\dagger\hat{a}_i$ $\left(\hat{n}_{bi} = \hat{b}_i^\dagger\hat{b}_i\right)$ denotes the particle number operator, the inter-well tunnelling strengths of two components between two wells are assumed constants, the intraspecies interaction strengths U_a and U_b are all constants, and the interspecies interaction strength U_{ab} is also a constant.

As is well known, the emergence of PS in one well needs large repulsive interaction due to competition between interaction energy and kinetic energy. Therefore, in some range of small repulsive interaction, the PS may not occur. Fortunately, in our paper, we consider only weak repulsive interaction between components, so PS in each well does not occur.

In the mean-field approximation $\langle\hat{a}\rangle = a$ ($\langle\hat{b}\rangle = b$) with a (b) being the c number, the Heisenberg equations give rise to the following equations:

$$\mathrm{i}\dot{a}_j = -T_a\sum_i a_i + (U_a|a_j|^2 + U_{ab}|b_j|^2 + T_a)a_j \tag{2}$$

$$\mathrm{i}\dot{b}_j = -T_b\sum_i b_i + (U_b|b_j|^2 + U_{ab}|a_j|^2 + T_b)b_j \tag{3}$$

where $j = 1, 2, 3$, the overhead dot denotes the time derivative, $\sum_i |a_i|^2 = 1$ and $\sum_i |b_i|^2 = 1$. Three wells are assumed to be identical and each well can be approximately determined by a harmonic potential. We can define a characteristic length $l = \sqrt{\frac{\hbar}{m_a\omega}}$, where m_a is the atomic mass for component a, and ω is the harmonic oscillation frequency, which is dependent on the shape of the well and the distance between every two wells. Then the dimensionless variables in the above equations can be obtained by the transformations $t = \omega^{-1}t'$, $\mathbf{r} = l\mathbf{r}'$, $U_a = \frac{4\pi a_a N_a}{l}U_a'$, $U_b = \frac{4\pi a_b N_b k}{l}U_b'$, $U_{ab} = \frac{4\pi a_{ab}N_b(1+k)}{l}U_{ab}'$, $T_a = \hbar\omega T_a$ and $T_b = \hbar\omega T_b$, where $k = m_a/m_b$, and N_a and N_b are the total number of particles for components a and b. a_a and a_b are the s-wave scattering lengths for components a and b, respectively, a_{ab} is the s-wave scattering length between atoms a and b. The spatial parts of wavefunctions for the components a and b are normalized by $\sqrt{\frac{N_a}{l^3}}$ and $\sqrt{\frac{N_b}{l^3}}$, respectively. The superscripts of variables have been omitted in equations (2) and (3).

In this paper, we concentrate on the ground state of BEC mixtures; therefore, we start with the time-independent coupled GPEs, written in the following form:

$$\mu_a a_i = -T_a\sum_{j\neq i} a_j + (U_a|a_i|^2 + U_{ab}|b_i|^2)a_i \tag{4}$$

$$\mu_b b_i = -T_b\sum_{j\neq i} b_j + (U_b|b_i|^2 + U_{ab}|a_i|^2)b_i \tag{5}$$

where $\mu_{a,b}$ are chemical potentials of the two components. Solving numerically the above nonlinear equations together with total particle conservation conditions $\sum_i |a_i|^2 = 1$ and $\sum_i |b_i|^2 = 1$, we readily obtain the ground state $(a_1, a_2, a_3, b_1, b_2, b_3)$ of the system which consists of the symmetric state ($x_i = x_j = x_k = \frac{1}{\sqrt{3}}, x = a, b$) and asymmetric state ($x_i = x_j \neq x_k, x = a, b$).

For the symmetric state (SS), every well is occupied by the same number of bosons for both components. For the asymmetric state, three cases are thus obtained through index permutation due to the symmetry of triple wells, $x_1 = x_2 \neq x_3$, $x_1 = x_3 \neq x_2$, $x_2 = x_3 \neq x_1$. For generality and simplicity, we consider only one of the above cases, $x_1 = x_2 \neq x_3$.

If we let $x_1 = x_2 = x$, $x_3 = S_x$, then the asymmetric ground state can be expressed by (a, a, S_a, b, b, S_b). Two different cases exist as follows.

(1) $S_a > a$ and $S_b > b$. In this case, the ground state is in the ST state. Two components coexist in the same well.
(2) $S_a < a$ and $S_b > b$ (or $S_a > a$ and $S_b < b$). In this case the ground state is in the PS state. Two components repel each other. If $S_a = a$ and $S_b = b$, it is only the symmetric case mentioned above. Three configurations of the ground state are shown schematically in figure 1.

3. Phase diagram and phase transition

We sweep the $\{U_b, U_{ab}\}$ parameter space in a large range with different values of the parameters U_a, T_a, T_b and obtain the phase diagram of the ground state as shown in figure 2. The phase diagram is divided into three regions, corresponding to three configurations of the SS phase, ST phase and PS phase, respectively. The thin line denotes the continuous transition between the ST phase and the PS phase, while the thick curve denotes a first-order phase transition between the ST state and the SS state or between the PS state and the SS state. Point S is a three-phase point where the ST phase, PS phase and SS phase meet together.

The phase diagrams of the ground state for different values of U_a are shown in figure 3(a), where $U_a = -0.1, 0.5$ respectively which are different from that in figure 2; the other

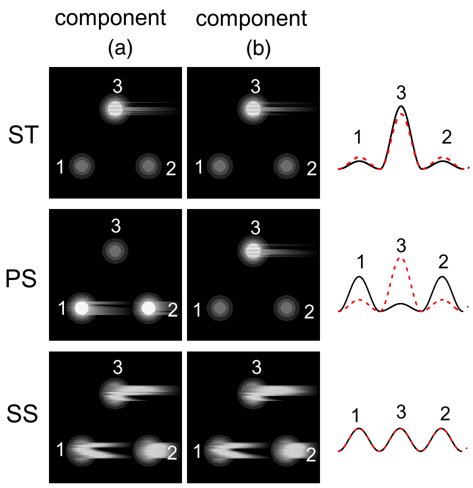

Figure 1. Schematic drawing, showing three configurations of the ground state. The black solid line indicates the component a, while the red dashed line denotes the component b.

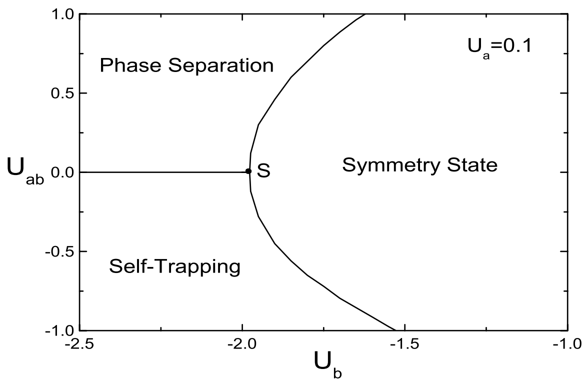

Figure 2. The phase diagram of the ground state for a two-component triple-well system in the plane of the intra-species interaction strength U_b and the inter-species interaction strength U_{ab}, showing the regions of the PS phase, ST phase, and SS phase. Here $U_a = 0.1$, $T_a = T_b = 0.5$.

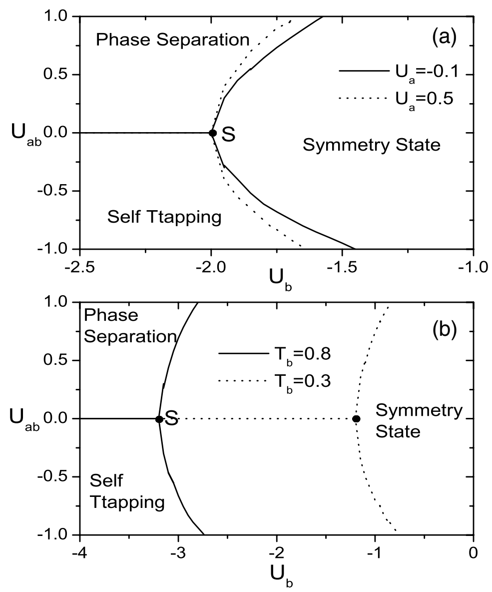

Figure 3. The phase diagram of the ground state for a two-component triple-well system in the plane of the intra-species interaction strength U_b and the inter-species interaction strength U_{ab}, showing the regions of the PS phase, ST phase, and SS phase. (a) The solid line represents the case of $U_a = -0.1$, $T_a = T_b = 0.5$, the dashed line represents the case of $U_a = 0.5$, $T_a = T_b = 0.5$, (b) the solid line represents the case of $U_a = 0.1$, $T_a = 0.5$, $T_b = 0.8$, and the dashed line represents the case of $U_a = 0.1$, $T_a = 0.5$, $T_b = 0.3$.

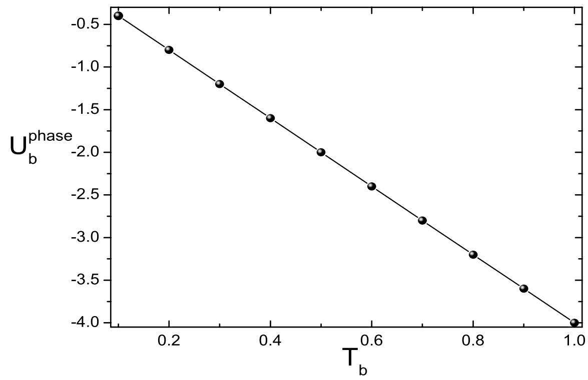

Figure 4. The dependence of U_b^{phase} on T_b, where $U_{ab} = 0$, $U_a = 0.1$.

parameters are the same as those in figure 2. Other many different values of U_a are taken and simulated. From these numerical results, we know that the three-phase point S is almost independent of U_a.

Similarly the phase diagrams of the ground state for different values of $T_a = 0.3, 0.8$ are shown in figure 3(b), respectively. The other parameters are the same as those in figure 2. They show that the three-phase point S depends on T_b. If the three-phase point S is denoted by $(U_b, U_{ab}) = \left(U_b^{\text{phase}}, 0\right)$, we find that U_b^{phase} decreases as T_b increases. The dependence of U_b^{phase} on T_b is shown in figure 4.

In the following we choose the variables of both $|S_a|^2$ and $|S_b|^2$ (the occupation in the third well for the two components a and b, respectively) and try to know how they vary when they cross the phase boundary.

3.1. The first-order phase transition between the asymmetric state and the SS state

(1) *Phase transition between the ST state and the SS state.* In figure 5, $|S_a|^2$ and $|S_b|^2$ are plotted as functions of U_b from the ST state to the SS state, where $U_{ab} = -0.8$ is fixed. We take $U_a = -0.1$ and 0.5 in figures 5(a) and (b), respectively. Meanwhile, we take $T_a = 0.3$ and 0.8 in figures 5(c) and (d), respectively; the other system parameters are the same.

These figures show that $|S_a|^2$ and $|S_b|^2$ decrease as U_b increases. At the critical point of the phase boundary, both curves suddenly jump to $\frac{1}{3}$. This behaviour reflects the fact that the occupation number in the third well has a sudden change at the critical point. It indicates that a first-order phase transition occurs from the ST state to the SS state since the curve is not continuous at the critical point.

After further numerical simulations with lots of different values of the parameters of U_a and T_b, we find that the critical point is nearly independent of

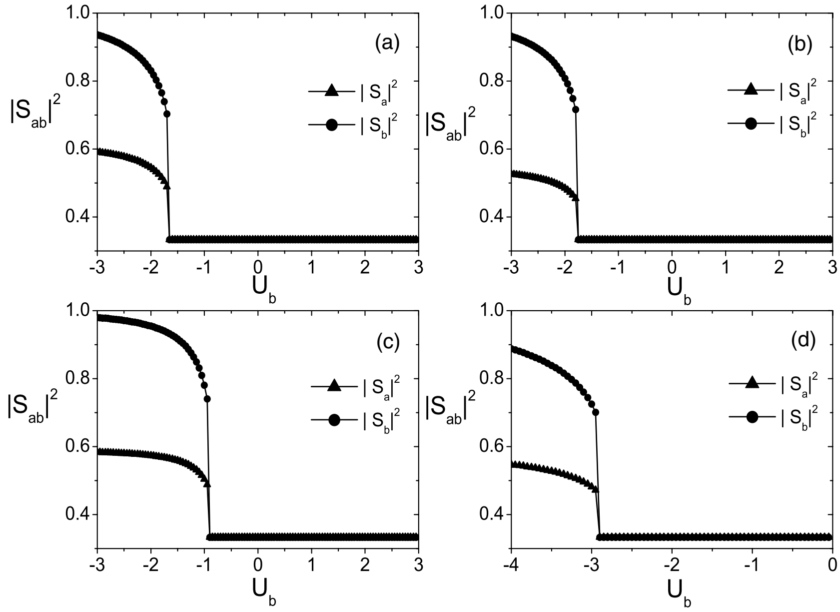

Figure 5. $|S_a|^2$ and $|S_b|^2$ versus U_b from the ST phase to the SS phase at $U_{ab} = -0.8$. (a) $U_a = -0.1$, $T_a = T_b = 0.5$, (b) $U_a = 0.5$, $T_a = T_b = 0.5$, (c) $U_a = 0.1$, $T_a = 0.5$, $T_b = 0.3$, (d) $U_a = 0.1$, $T_a = 0.5$, $T_b = 0.8$.

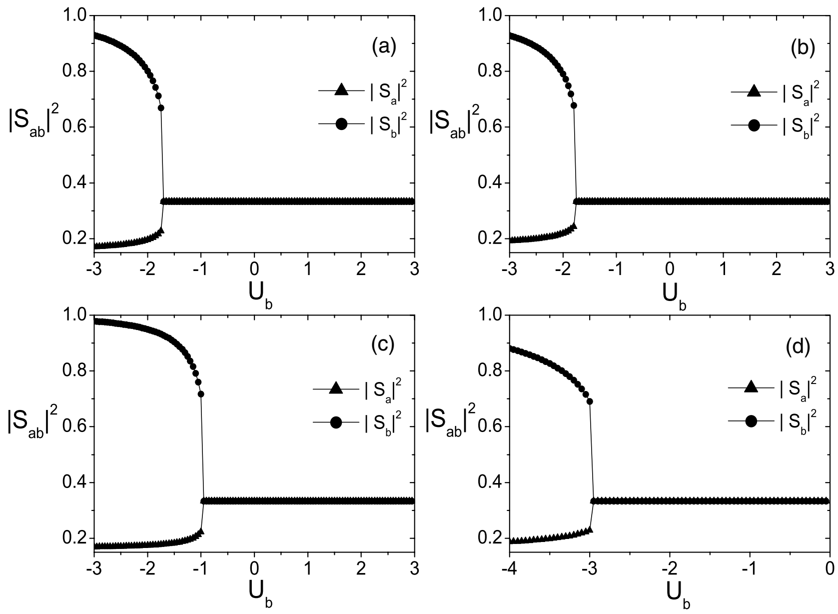

Figure 6. $|S_a|^2$ and $|S_b|^2$ versus U_b from the PS phase to the SS phase at $U_{ab} = 0.8$. (a) $U_a = -0.1$, $T_a = T_b = 0.5$, (b) $U_a = 0.5$, $T_a = T_b = 0.5$, (c) $U_a = 0.1$, $T_a = 0.5$, $T_b = 0.3$, (d) $U_a = 0.1$, $T_a = 0.5$, $T_b = 0.8$.

U_a; however, it depends on T_b. The critical point U_b^{cri} decreases as T_b increases. We conclude that the dependences of the critical point U_b^{cri} on the parameters U_a and T_b are similar to those of the three-phase point U_b^{phase}.

(2) *Phase transition between the PS state and the SS state.* In this case, we fix $U_{ab} = 0.8$. The dependences of both $|S_a|^2$ and $|S_b|^2$ on U_b are plotted in figure 6. It is noted that as U_b increases, $|S_b|^2$ decreases while $|S_a|^2$ increases. At the critical point, both $|S_b|^2$ and $|S_a|^2$ suddenly jump to $\frac{1}{3}$. It seems that the phase transition between the PS state and the SS state is similar to that between the ST state and the SS state, which indicates that it is a first-order phase transition since it is not continuous at the critical point.

It is also noted from the other different parameters of U_a and T_b that the critical point is nearly independent of U_a (see figures 6(a) and (b)); however, it depends on T_b. The critical point U_b decreases as T_b increases (see figures 6(c) and (d)).

3.2. The continuous phase transition between the ST state and the PS state

Figure 7 shows the dependences of both $|S_a|^2$ and $|S_b|^2$ on the parameter of U_{ab} between the ST state and the PS state where

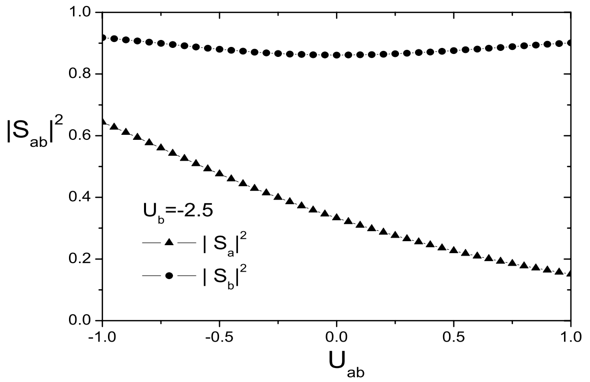

Figure 7. $|S_a|^2$ and $|S_b|^2$ versus U_{ab} from the ST phase to the PS phase at $U_b = -2.5$. Here $U_a = 0.1$, $T_a = T_b = 0.5$.

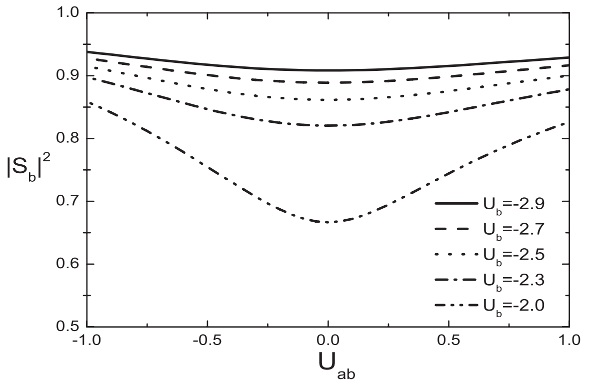

Figure 8. (a) $|S_b|^2$ versus U_{ab} from the ST phase to the PS phase with different U_b. Here $U_a = 0.1$, $T_a = T_b = 0.5$.

$U_b = -2.5$. We find that both $|S_a|^2$ and $|S_b|^2$ decrease as U_{ab} increases at first, but $|S_a|^2$ drops sharper than $|S_b|^2$ until at the critical point $U_{ab} = 0$.

At the critical point $U_{ab} = 0$, $|S_b|^2$ reaches its minimum. By further increasing U_{ab}, $|S_b|^2$ begins to increase gradually, while $|S_a|^2$ continues to decline. At this point, the system enters the regime of PS.

The variations of $|S_b|^2$ with respect to U_{ab} for different $U_b = -2.9, -2.7, -2.5, -2.3, -2$ are plotted in figure 8. It is found that all curves display the similar behaviour as that in figure 7. $|S_b|^2$ decreases first as U_{ab} increases, and then reaches its minimum value at a critical point $U_{ab} = 0$. It increases as U_{ab} increases further in the region of $U_{ab} > 0$.

In order to know the phase transition in more detail, the variation of $|S_b|^2$ against the parameter U_{ab} is considered again. We note that $|S_b|^2$ is a continuous function of U_{ab} and find power law scalings at the point $U_{ab}^c = 0$ as follows:

$$|S_b(U_{ab})|^2 - \left|S_b\left(U_{ab}^c\right)\right|^2 \propto \left(U_{ab}^c - U_{ab}\right)^\alpha, \qquad U_{ab} < U_{ab}^c \tag{6}$$

$$|S_b(U_{ab})|^2 - \left|S_b\left(U_{ab}^c\right)\right|^2 \propto \left(U_{ab} - U_{ab}^c\right)^\beta, \qquad U_{ab} > U_{ab}^c. \tag{7}$$

The dependences of both α and β on the parameter U_b are approximately equal to 2, i.e. $\alpha \approx \beta \approx 2$. This suggests that the phase transition from ST to PS is a continuous transition.

4. Conclusion

The phase diagram of the ground state of two-component BECs in a triple-well trap system is studied in this paper. There are three regions in the phase space for this system, the symmetry state (SS) phase, self-trapping (ST) phase and phase separation (PS) phase, which depend on the parameters of interaction strength. There are two kinds of phase transitions. One is the first-order transition such as the SS state to the ST state, or the SS to the PS state. The other transition is from the ST state to the PS state which is a continuous phase transition.

From the ST phase to the SS state, the occupation probabilities of both components in the third well decrease monotonically as the intraspecies interaction strength increases until it reaches a critical point at the phase boundary, and then both occupation probabilities become 1/3 (the SS state is reached).

Similarly, from the PS phase to the SS state, one of the occupation probabilities of the components in the third well decreases monotonically, while the other increases monotonically as the intraspecies interaction strength increases until it reaches a critical point at the phase boundary, and then both occupation probabilities suddenly become 1/3 (the SS state is reached).

The phase transition from the ST phase to the PS phase is a continuous transition. The phase transition point is a point where interspecies interaction strength is zero. At this point, the power law scaling is obtained.

The three-phase point phase transition between the ST state and the SS state and the phase transition between the PS state and the SS state are all nearly independent of the intraspecies interaction strength; however, they all depend on the inter-well tunnelling strength of the two components.

It will be interesting to investigate the detailed dynamics (e.g. time evolution) of the phase transitions if the system parameters such as intraspecies or interspecies interaction strength are time dependent. We also plan to generalize this work to the asymmetric open trimer made of three coupled BECs arranged into a row.

Acknowledgments

The work was supported by the National Natural Science Foundation of China (no 91021021, 11075020, 10725521, 10875098), the National Fundamental Research Programme of China under grant no 2011CB921503, 2007CB814800, and the Natural Science Foundation of Northwest Normal University (grant no NWNU-KJCXGC-03-48).

References

[1] Ho T L and Shenoy V B 1996 *Phys. Rev. Lett.* **77** 3276
Ao P and Chui S T 1998 *Phys. Rev.* A **58** 4836
[2] Wu Y S 2003 *Phys. Rev.* A **67** 013606
Chui S T and Ao P 1999 *Phys. Rev.* A **59** 1473
Esry B D and Greene C H 1999 *Phys. Rev.* A **59** 1457
[3] Law C K, Pu H, Bigelow N P and Eberly J H 1998 *Phys. Rev.* A **58** 531
[4] Law C K, Pu H, Bigelow N P and Eberly J H 1997 *Phys. Rev. Lett.* **79** 3105

[5] Williams J *et al* 1999 *Phys. Rev.* A **59** R31
[6] Trippenbach M, Band Y B and Julienne P S 2000 *Phys. Rev.* A **62** 023608
[7] Molmer K 1998 *Phys. Rev. Lett.* **80** 1804
[8] Modugno G, Modugno M, Riboli F, Roati G and Inguscio M 2002 *Phys. Rev. Lett.* **89** 190404
[9] Burke J P *et al* 1998 *Phys. Rev. Lett.* **80** 2097
Kokkelmans S, Verhaar B J and Gibble K 1998 *Phys. Rev. Lett.* **81** 951
[10] Myatt C J *et al* 1997 *Phys. Rev. Lett.* **78** 586
Hall D S *et al* 1998 *Phys. Rev. Lett.* **81** 539
Hall D S, Matthews M R, Wieman C E and Cornell E A 1998 *Phys. Rev. Lett.* **81** 1543
[11] Stamper-Kurn D M *et al* 1998 *Phys. Rev. Lett.* **80** 2027
[12] Thalhammer G *et al* 2008 *Phys. Rev. Lett.* **100** 210402
[13] Ng H T, Law C K and Leung P T 2003 *Phys. Rev.* A **68** 013604
[14] Wen L H and Li J H 2007 *Phys. Lett.* A **369** 307
[15] Ashhab S and Lobo C 2002 *Phys. Rev.* A **66** 013609
[16] Pu H, Zhang W P and Meystre P 2002 *Phys. Rev. Lett.* **89** 090401
[17] Müstecaplıoğlu Ö E, Zhang W X and You L 2007 *Phys. Rev.* A **75** 023605
[18] Xu X Q, Lu L H and Li Y Q 2008 *Phys. Rev.* A **78** 043609
Jiang X, Duan W S, Li S C and Shi Y R 2009 *J. Phys. B: At. Mol. Opt. Phys.* **42** 185001
[19] Qiu H, Tian J and Fu L-B 2010 *Phys. Rev.* A **81** 043613
[20] Liu B, Fu L B, Yang S P and Liu J 2007 *Phys. Rev.* A **75** 033601
Wang G F, Ye D F, Fu L B, Chen X Z and Liu J 2006 *Phys. Rev.* A **74** 033414
[21] Buonsante P, Franzosi R and Penna V 2003 *Phys. Rev. Lett.* **90** 050404
Franzosi R and Penna V 2003 *Phys. Rev.* E **67** 046227
[22] Lee C, Alexander T J and Kivshar Y S 2006 *Phys. Rev. Lett.* **97** 180408
[23] Raghavan S, Smerzi A, Fantoni S and Shenoy S R 1999 *Phys. Rev.* A **59** 620
[24] Ananikian D and Bergeman T 2006 *Phys. Rev.* A **73** 013604
[25] Satija I I, Balakrishnan R, Naudus P, Heward J, Edwards M and Clark C W 2009 *Phys. Rev.* A **79** 033616
[26] Liu J, Wu B and Niu Q 2000 *Phys. Rev.* A **61** 023402
Fu L B, Liu J and Chen S G 2002 *Phys. Lett.* A **298** 388
[27] Ye D F, Fu L B and Liu J 2008 *Phys. Rev.* A **77** 013402
[28] Fu L B and Liu J 2006 *Phys. Rev.* A **74** 063614